




Repurposing of chloroquine and some clinically approved antiviral drugs as effective therapeutics to prevent cellular entry and replication of coronavirus

Akinwunmi O. Adeoye^a, Babatunde Joseph Oso^b , Ige Francis Olaoye^b, Habibu Tijjani^c and Ahmed I. Adebayo^d

^aDepartment of Biochemistry, Federal University Oye-Ekiti, Oye-Ekiti, Nigeria; ^bDepartment of Biochemistry, McPherson University, Seriki Sotayo, Nigeria; ^cDepartment of Biochemistry, Natural Product Research Laboratory, Bauchi State University, Gadau, Nigeria; ^dDepartment of Biochemistry, University of Ilorin, Ilorin, Nigeria

Communicated by Ramaswamy H. Sarma

ABSTRACT

The reemergence of coronavirus prompts the need for the development of effective therapeutics to prevent the cellular entry and replication of coronavirus. This study demonstrated the putative inhibitory potential of lopinavir, remdesivir, oseltamir, azithromycin, ribavirin, and chloroquine towards V-ATPase, protein kinase A, SARS-CoV spike glycoprotein/ACE-2 complex and viral proteases. The pharmacodynamic and pharmacokinetic properties were predicted through the pkCSM server while the corresponding binding affinity of the selected drugs towards the proteins was computed using AutodockVina Screening tool. The ADMET properties revealed all the drugs possess drug-like properties. Lopinavir has the highest binding affinities to the pocket site of SARS-CoV spike glycoprotein/ACE-2 complex, cyclic AMP-dependent protein kinase A and 3-Chymotrypsin like protease while redemsvir has the highest binding affinities for vacuolar proton-translocating ATPase (V-ATPase) and papain-like proteins. The amino acids Asp269, Leu370, His374, and His345 were predicted as the key residues for lopinavir binding to human SARS-CoV spike glycoprotein/ACE-2 complex while His378, Tyr515, Leu73, Leu100, Phe32 and Phe40 for remdesivir and Tyr510, Phe504, Met62, Tyr50, and His378 were predicted for azithromycin as the key residues for binding to SARS-CoV spike glycoprotein/ACE-2 complex. Moreover, it was also observed that chloroquine has appreciable binding affinities for 3-Chymotrypsin-like protease and cyclic AMP-dependent protein kinase A when compared to Oseltamivir and ribavirin. The study provided evidence suggesting putative repurposing of the selected drugs for the development of valuable drugs for the prevention of cellular entry and replication of coronavirus.

ARTICLE HISTORY

Received 24 April 2020
Accepted 1 May 2020

KEYWORDS

Coronavirus; antiviral drugs; chloroquine; Autodock tool; pkCSM tool

1. Introduction

Coronaviruses have long been recognized as important veterinary pathogens, causing respiratory and enteric diseases in mammals as well as in birds. They are single-stranded RNA viruses that belong to the order Nidovirales, family Coronaviridae, and subfamily Coronavirinae. About twenty-six different species have been identified (Cleri et al., 2010) and are classified into four types (alpha, beta, gamma, and delta). They are characterized by different antigenic cross-reactivity and genetic makeup (Paules et al., 2020). From the various species of coronavirus, only six have been reported to cause disease in humans. These include HCoV-229E, HCoV-OC43, HCoV-NL63, HCoV-HKU1, severe acute respiratory syndrome coronavirus (SARS-CoV) and Middle East respiratory syndrome coronavirus (MERS-CoV) (Arabi et al., 2017; Skariyachan et al., 2019). SARS-CoV and MERS-CoV are beta coronaviruses, and are among the pathogens included in the World Health Organization's list of high-priority threats (Zumla et al., 2015). In late 2019, a novel coronavirus (COVID-19) initially designated as 2019-nCoV was discovered to be the cause of a large and rapidly spreading outbreak of

respiratory disease, including pneumonia. According to the isolation and viral genome sequence, coronavirus was identified as a beta-coronavirus belonging to group 2B with at least 70% similarity in genetic sequence to SARS-CoV (Hui et al., 2020), and thus became the seventh discrete coronavirus species capable of causing human disease.

Recently, chloroquine, a medication used primarily to treat malaria, is being studied to treat coronavirus. Its putative anti-viral effects have been hypothesized to be related to the elevation of endosomal and lysosomal pH in addition to its angiotensin-converting enzyme 2 inhibitory potentials (Vincent et al., 2005; Gay et al., 2012). Unlike viruses such as human immunodeficiency virus and herpes simplex virus, Sendai virus that can fuse the plasma membrane to successfully infect the host, enveloped viruses such as coronaviruses are endocytosed in the endosome and lysosome before fusion aiding its entry into cells (Plempner, 2011; Boopathi et al., 2020). Lysosomal lumens are the most acidic subcellular structure of the cell, pH ~4.5. Acidification of the lysosomal lumen activates hydrolytic enzymes which lead to the degradation of endocytic cargo (Ishida et al., 2013). However, changes in the environment of the lysosome such as a

decrease in pH could elicit conformational changes of viral glycoproteins and proteolytic activation of viral glycoproteins by endosomal proteases leading to virions maturation and viral fusion with the host membranes changes (Huotari & Helenius, 2011; Richards & Jackson, 2012; Park et al., 2014). Acidification of the lysosomal lumen could enhance the cellular entry of coronavirus. Thus, intracellular extrusion of the proton through modulations of the functions of membrane proton pumps could enhance the elevation of endocytic pH and inhibit viral fusion and subsequent replication in the host.

Proton pumps that have been implicated in endocytic acid-base balance include vacuolar proton-translocating ATPase (V-ATPase) and Na/H exchangers (NHE). V-ATPase is a membrane-bound protein that is required to pump protons into the lysosomal lumen and maintain an acidic luminal pH. Inhibition of the host V-ATPase has been shown to result in a decrease of lysosomal acidification (Slesiona et al., 2012). Conversely, NHE modulates the luminal pH and Na⁺ homeostasis by transporting protons out of the lysosomal lumen in exchange for cations, hence increasing the luminal pH (Nakamura et al., 2005; Prasad & Rao, 2015). Regulation of NHE is mediated by protein kinase A through phosphorylation to sustained intracellular acidosis (Zhao et al., 1999; Haworth et al., 2003). Therefore, endocytic acidification could be dissipated through inhibition of protein kinase A.

Moreover, binding of the S1 domain of the SARS-CoV-2 spike protein to human angiotensin-converting enzyme 2 (ACE2) is a key event in the cellular entry of SARS-CoV-2 (Li et al., 2003). ACE2 is a type I integral membrane glycoprotein with an N-terminal extracellular domain comprising 2 α -helical lobes, which has a catalytic site with a coordinated zinc ion between the lobes (Li et al., 2003). Increasing numbers of proteases have been demonstrated to participate in viral infection of host cells in mechanisms where they do not act as receptors. These proteases are reported to be involved not only in the adaptation of the virus to innate immune response but also in proteolytic processing of the S protein. Coronaviruses always produce two types of cysteine proteases, a chymotrypsin-like main protease and papain-like proteases (PL1pro and PL2pro) which are generally important for viral entry and replication (Elmezayen et al., 2020; Khan et al., 2020a; Muralidharan et al., 2020). The fusion of coronavirus requires proteolytic priming of its spike protein in the endosomal system. Besides, inhibition of lysosomal proteases had been hypothesised to prevent coronavirus fusion as shown in a study using mouse hepatitis virus (MHV) a safe model of coronavirus (de Haan et al., 2004; Hasan et al., 2020; Joshi et al., 2020). Various studies had been reported using computational approaches in investigating putative compounds that could be repurposed or repositioned as drugs against coronavirus (Aanouz et al., 2020; Elfiky & Azzam, 2020; Enayatkhani et al., 2020; Enmozhi et al., 2020; Gupta et al., 2020; Khan et al., 2020b; Sarma et al., 2020). Several classes of compounds that had been proposed include phytochemicals and peptides (Aanouz et al., 2020; Pant et al., 2020).

In a quest to identifying potential treatment for the novel coronavirus infection, this study demonstrated the putative repurposing of some selected clinically approved drugs (lopinavir, remdesivir, oseltamir, azithromycin, ribavirin, and chloroquine recently discovered) as inhibitors of V-ATPase, protein kinase A, human angiotensin-converting enzyme 2 and viral proteases through *in silico* analyses.

2. Materials and methods

2.1. ADMET studies

The toxicity risks of azithromycin, chloroquine, lopinavir, oseltamivir, remdesivir, and ribavirin were predicted based on their ADMET profile. The ADMET (absorption, distribution, metabolism, elimination, and toxicity) studies were predicted using pkCSM tool (<http://biosig.unimelb.edu.au/pkcsm/prediction>) (Pires et al., 2015). The SMILE molecular structures of the compounds were obtained from PubChem (<https://pubchem.ncbi.nlm.nih.gov>).

2.2. Protein preparation

The crystal structures of papain-like protease (PLpro), chymotrypsin-like protease (3CLpro), SARS coronavirus spike glycoprotein-angiotensin converting enzyme 2 complex (SARS-CoV spike glycoprotein/ACE-2 complex), cyclic AMP-dependent protein kinase A (cAMP-PKA) and V-ATPase with PDB IDs 2FE8, 2ALV, 2AJF, 4UJ1, and 511M respectively were retrieved from the protein databank (www.rcsb.org) (Berman et al., 2000). All the crystal structures were prepared individually by removing existing ligands and water molecules, while missing hydrogen atoms were added using Autodock v4.2 program, Scripps Research Institute. Thereafter, non-polar hydrogens were merged while polar hydrogen were added to each enzyme. The process was repeated for each protein and subsequently saved into pdbqt format in preparation for molecular docking.

2.3. Ligand preparation

The SDF structures of azithromycin, chloroquine, lopinavir, oseltamivir, remdesivir, and ribavirin were retrieved from the PubChem database (www.pubchem.ncbi.nlm.nih.gov) (Kim et al., 2019). The compounds were converted to mol2 chemical format using Open babel (O'Boyle et al., 2011). Polar hydrogens were added while non-polar hydrogens were merged with the carbons and the internal degrees of freedom and torsions were set. The protein and ligand molecules were further converted to the dockable pdbqt format using Autodock tools.

2.4. Molecular docking

Docking of the ligands to various protein targets and determination of binding affinities was carried out using AutodockVina (Trott & Olson, 2010). Pdbqt format of the receptors, as well as those of the ligands, was dragged into

Table 1. Predicted molecular and absorption properties of the proposed drugs.

Model Name	Azithromycin	Chloroquine	Lopinavir	Oseltamivir	Remdesivir	Ribavirin
Lipophilicity (LogP)	1.9007	4.8106	4.32814	1.2854	2.31218	-3.0115
Water solubility (log mol/L)	-4.133	-4.249	-4.819	-2.471	-3.07	-1.712
Caco2 permeability (log Papp in 10 ⁻⁶ cm/s)	-0.211	1.624	0.063	0.934	0.635	0.421
Human intestinal absorption (%)	45.808	89.95	65.607	74.469	71.109	54.988
Skin Permeability (log Kp)	-2.742	-2.679	-2.736	-3.177	-2.735	-2.763
P-glycoprotein substrate	Yes	Yes	Yes	No	Yes	No
P-glycoprotein I inhibitor	Yes	No	Yes	No	Yes	No
P-glycoprotein II inhibitor	No	No	Yes	No	No	No

Caco2=Human colon adenocarcinoma-2

their respective columns and the software was run. The binding affinities of compounds for the three protein targets were recorded. The compounds were then ranked by their affinity scores. Molecular interactions between the receptors and compounds with most remarkable binding affinities were viewed with Discovery Studio Visualizer, BIOVIA, 2016. The respective binding free energy was calculated by the Molecular Mechanics/Generalized Born Surface Area (MM/GBSA) using HawkDock Server (<http://cadd.zju.edu.cn/hawk-dock/>) (Chen et al., 2016).

2.5. Molecular dynamics simulation

The conformational stability of the protein-ligand interactions was evaluated using molecular dynamics simulations analysis performed through iMODS server (<http://imods.chaconlab.org>) by normal mode analysis (NMA) predicting properties such as deformability, mobility profiles, eigenvalues, variance, co-variance map and elastic network of the protein-ligand interactions (López-Blanco et al., 2014).

3. Results and discussion

The results of the predicted pharmacokinetics and pharmacodynamics properties of the azithromycin, chloroquine, lopinavir, oseltamivir, remdesivir, and ribavirin are presented in Tables 1–5. The prediction was carried out as a methodological virtual screening of the drugs. It was included as a substitute to *in vivo* studies which are important complements in drug discovery. The molecular properties of the drugs based on the computed partition coefficient (log P) showed that the drugs had relatively good lipophilicity as the logP values were less than 5 (Lipinski et al., 1997; Hughes et al., 2008) (Table 1). However, a negative ribavirin logP value means the ribavirin is a hydrophilic drug that could negatively impact permeability. Since high lipophilic drugs which are insoluble in aqueous layers could be poorly absorbed and hydrophilic drugs could also contribute to poor permeability, all the screened drugs except ribavirin could be maintained in the system at appropriate concentrations. Moreover, the observed lipophilicities correlated negatively with water solubility potentials of the drugs but had an association with Caco2 permeability. This corresponds to the observation of Yazdani et al. (1998) that there was no correlation between the lipophilicity and drug permeability measured using the human colon adenocarcinoma (Caco-2) cell line assay. Caco2 permeability and intestinal absorption (HIA) indices are factors that determine the ultimate

bioavailability of the drug. The drugs had relatively low Caco2 permeability potential ($<8 \times 10^{-6}$ cm/s) and could be absorbed through the human intestine (Larregieu & Benet, 2013). However, the drugs that have their subcellular localization in the lysosome are remdesivir, azithromycin, and chloroquine as predicted by ADMETSAR1 (Cheng et al., 2012). Lopinavir, remdesivir, azithromycin, and chloroquine were predicted to be substrates of P-glycoprotein, an efflux membrane transporter and a member of the ATP-binding cassette transporter found primarily in epithelial cells. However, lopinavir, remdesivir, and azithromycin were also predicted as P-glycoprotein inhibitors. Thus, lopinavir, remdesivir, and azithromycin could modulate the physiological functions of P-glycoprotein in limiting the active uptake and the distribution of drugs (Srivalli & Lakshmi, 2012).

The prediction through the volume of distribution calculated using a steady-state volume of distribution (VD_{ss}) showed that lopinavir, azithromycin, and ribavirin had lower theoretical dose required for uniform distribution in the plasma than remdesivir, oseltamivir, and chloroquine while the degree of diffusing across plasma membrane increases in this order lopinavir < remdesivir < chloroquine < azithromycin < oseltamivir < ribavirin measured as the fraction that is in the unbound state (Table 2). The predictive assessment of the distribution of the drugs through the nervous system showed that lipophilicity of the drugs correlates to the tendency to permeate the blood-brain barrier and the central nervous system passively. Moreover, the moderate levels of the lipophilicity imply the drugs would have no negative effect on nervous system exposure.

Furthermore, a group of enzymes that play significant roles in drug metabolism is the CYP isozymes. Oseltamivir and ribavirin showed low CYP promiscuity while lopinavir, remdesivir, azithromycin, and chloroquine are substrates of CYP3A4 (Table 3). The lipophilicity of the drug appears to correlate negatively to metabolism-related toxicity. Lopinavir has the highest CYP promiscuity as it inhibits CYP2C19, CYP2C9, CYP2D6, and CYP3A4. This shows that lopinavir could be involved in drug-drug interaction (Cheng et al., 2011). However, it could also alleviate the generation of oxidative species CYP2C9, CYP2C19, CYP2D6, and CYP3A4 and could initiate oxidative stress (Williams et al., 2004).

Also, only chloroquine was a substrate of renal organic cation transporter while other drugs are possibly cleared through other available routes such as bile, breath, faces, and sweat. It was observed from the results that all the drugs are absorbable via oral prescription (Table 4). The bacterial *mutagenic* potential of drugs through AMES toxicity testing showed that all the drugs except chloroquine could be considered as non-*mutagenic* agents. However, the

Table 2. Predicted in vivo distribution of the proposed drugs.

Model Name	Azithromycin	Chloroquine	Lopinavir	Oseltamivir	Remdesivir	Ribavirin
VDss (log L/kg)	-0.214	1.332	-0.248	0.043	0.307	-0.015
Fraction unbound	0.512	0.191	0.00	0.592	0.005	0.789
BBB permeability (log BB)	-1.857	0.349	-0.83	-0.693	-2.056	-0.921
CNS permeability (log PS)	-3.777	-2.191	-2.935	-3.111	-4.675	-3.756

VDss = Steady-state volume of distribution, BBB = Blood-brain barrier, CNS = Central nervous system.

Table 3. Predicted human cytochrome P450 promiscuity of the proposed drugs.

Model Name	Azithromycin	Chloroquine	Lopinavir	Oseltamivir	Remdesivir	Ribavirin
CYP2D6 substrate	No	Yes	No	No	No	No
CYP3A4 substrate	Yes	Yes	Yes	No	Yes	No
CYP1A2 inhibitor	No	No	No	No	No	No
CYP2C19 inhibitor	No	No	Yes	No	No	No
CYP2C9 inhibitor	No	No	Yes	No	No	No
CYP2D6 inhibitor	No	Yes	No	No	No	No
CYP3A4 inhibitor	No	No	Yes	No	No	No

Table 4. Predicted in vivo clearance of the proposed drugs.

	Azithromycin	Chloroquine	Lopinavir	Oseltamivir	Remdesivir	Ribavirin
Total Clearance (log ml/min/kg)	-0.424	1.092	0.459	0.923	0.198	0.623
Renal OCT2 substrate	No	Yes	No	No	No	No

OCT2 = Organic cation transporter 2.

Table 5. Predicted toxicological effects of the proposed drugs.

	Azithromycin	Chloroquine	Lopinavir	Oseltamivir	Remdesivir	Ribavirin
AMES toxicity	No	Yes	No	No	No	No
MTD (log mg/kg/day)	1.027	-0.167	-0.297	0.479	0.15	1.011
hERG inhibitor	No	Yes	Yes	No	Yes	No
ORAT (LD50) (mol/kg)	2.769	2.85	2.382	2.677	2.043	1.988
ORCT (log mg/kg_bw/day)	1.991	1.026	5.949	1.091	1.639	3.096
Hepatotoxicity	Yes	Yes	Yes	No	Yes	No
Skin Sensitization	No	No	No	No	No	No
<i>T.pyriformis</i> toxicity (log ug/L)	0.285	1.558	0.286	0.106	0.285	0.285
Minnow toxicity (log mM)	7.8	0.747	-1.501	2.31	0.291	4.626

AMES = *Salmonella typhimurium* reverse mutation assay, MTD = Maximum tolerated dose in human, hERG = Human ether-a-go-go-related gene, ORAT = Oral Rat Acute Toxicity, ORCT = Oral Rat Chronic Toxicity.

toxicities of all the drugs in *Tetrahymena pyriformis* were high. The acute toxicity assessed the predictive toxicity of the ligands and described the adversative effects that could occur within a short period after administration. Lopinavir, remdesivir, and chloroquine were also shown to have low toxic dose threshold in humans, inhibit human ether-a-go-go-related gene (hERG) and induce hepatotoxicity (Table 5). Thus, administration of lopinavir, remdesivir, and chloroquine could result in delayed ventricular repolarisation through inhibition of the hERG potassium channel which could lead to a severe disturbance in the normal cardiac rhythm and disrupt hepatic functions (Wang et al., 2012; Oso et al., 2019).

To comprehend the mechanism of ligand binding and to discover potent inhibitors of vacuolar proton-translocating ATPase (V-ATPase), cyclic AMP-dependent protein kinase A, SARS-CoV spike glycoprotein human angiotensin-converting enzyme 2 and viral proteases (3-Chymotrypsin like and papain-like protease), a virtual screening and molecular docking was carried out. The *in silico* studies on the molecular assessment on the possible interactions between drugs and the selected proteins showed that all the drugs had relatively good interaction with the proteins based on their

corresponding scoring values as specified by the negative values of the binding free energies (Oso & Olaoye, 2020) (Table 6). The binding free energy by MM/GBSA method is presented in Table 7.

Lopinavir has the highest binding affinities to the pocket site of SARS-CoV spike glycoprotein/ACE-2 complex, cyclic AMP-dependent protein kinase A and 3-Chymotrypsin like protease while remdesivir has the highest binding affinities for vacuolar proton-translocating ATPase (V-ATPase) and papain-like proteins. The observation from this study agrees with the work of Nukoolkarn et al. (2008), who reported that lopinavir showed a high binding ability to the pocket site of SARS-CoV. It was observed that lopinavir, remdesivir, and azithromycin have the highest docking scores with the highest number of hydrogen bonds formed respectively while ribavirin has the least docking score with the least hydrogen bonds. The calculated binding free energies using the MM/GBSA scoring showed that all the proposed drugs have favourable conformations as indicated by the empirical binding free energies with all the proteins except SARS-CoV spike glycoprotein/ACE-2 complex.

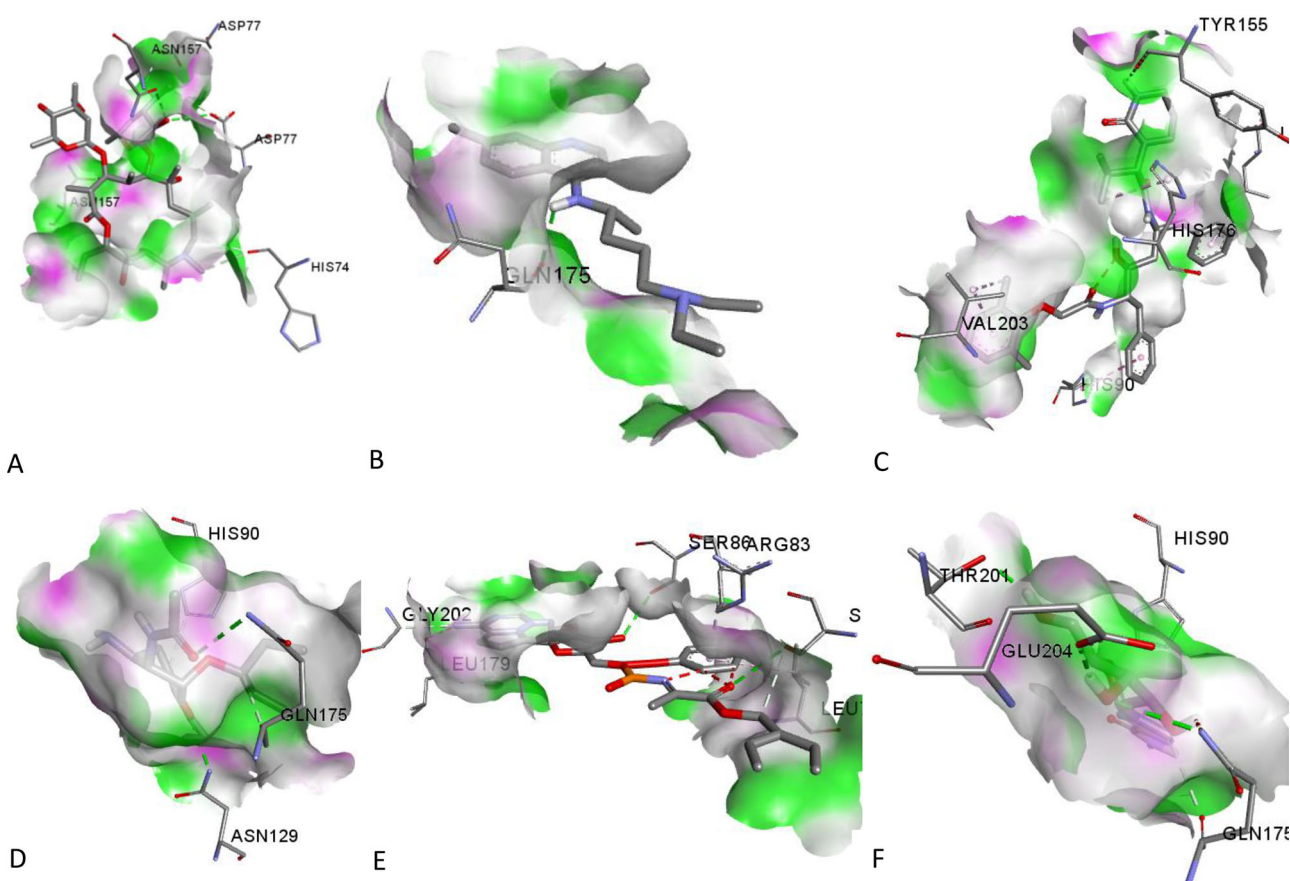
The molecular docking study also predicted the residues at the interacting site of the associated proteins and their

Table 6. Binding Affinity (Kcal/mol) of the drugs to 3CLpro, PLpro, SARS-CoV spike glycoprotein/ACE-2 complex, cAMP-PKA and V-ATPase.

S/N	Compounds	PLpro	3CLpro	SARS-CoV spike glycoprotein/ACE-2 complex	cAMP-PKA	V-ATPase
1	Azithromycin	-11.1	-9.8	-10.4	-10.7	-11.0
2	Chloroquine	-7.6	-7.2	-7.5	-8.6	-7.4
3	Lopinavir	-12.5	-10.7	-12.9	-12.2	-12.8
4	Oseltamivir	-7.7	-7.1	-8.0	-7.6	-7.9
5	Remdesivir	-12.7	-9.6	-12.3	-11.1	-13.9
6	Ribavirin	-7.7	-7.0	-7.0	-7.7	-7.5

Table 7. Binding free energy using MM/GBSA expressed in kcal/mol.

S/N	Compounds	PLpro	3CLpro	SARS-CoV spike glycoprotein/ACE-2 complex	cAMP-PKA	V-ATPase
1	Azithromycin	-45.50	-39.21	51.36	-124.04	-83.67
2	Chloroquine	-40.09	-37.39	51.36	-123.45	-78.96
3	Lopinavir	-39.11	-39.11	51.36	-122.82	-79.09
4	Oseltamivir	-39.67	-37.26	51.36	-125.37	-88.26
5	Remdesivir	-39.67	-36.71	51.36	-125.43	-82.86
6	Ribavirin	-40.84	-38.01	51.36	-123.92	-79.26

**Figure 1.** Docking view of the drugs in the binding sites of PLpro: (A) Azithromycin, (B) Chloroquine (C) Lopinavir (D) Oseltamivir, (E) Remdesivir, (F) Ribavirin.

corresponding orientations (Adeoye et al., 2019). The amino acids Asp269, Leu370, His374, and His345 were predicted to be the key residues for lopinavir binding to human SARS-CoV spike glycoprotein/ACE-2 complex while His378, Tyr515, Leu73, Leu100, Phe32 and Phe40 for remdesivir and Tyr510, Phe504, Met62, Tyr50, and His378 were predicted for azithromycin as the key residues for binding to SARS-CoV spike glycoprotein/ACE-2 complex (Figures 1–5 and Table 8).

The results suggest that the high number of hydrogen bond formation could be responsible for the high binding score in lopinavir, remdesivir, and azithromycin (Elokely &

Doerksen, 2013). Moreover, it was also observed that chloroquine which was recently found to be effective in the treatment of novel coronavirus infection has appreciable binding affinities for 3-Chymotrypsin-like protease and cyclic AMP-dependent protein kinase A when compared to Oseltamivir and ribavirin. This implies that chloroquine could limit the proliferation of coronavirus by enhancing the activities of Na/H exchangers leading to elevation of pH of the lysosomal lumen, and also limiting the effect of the viral proteases. Chloroquine could be used in the treatment remedy as it could be an inhibitor of the transporter that could reverse

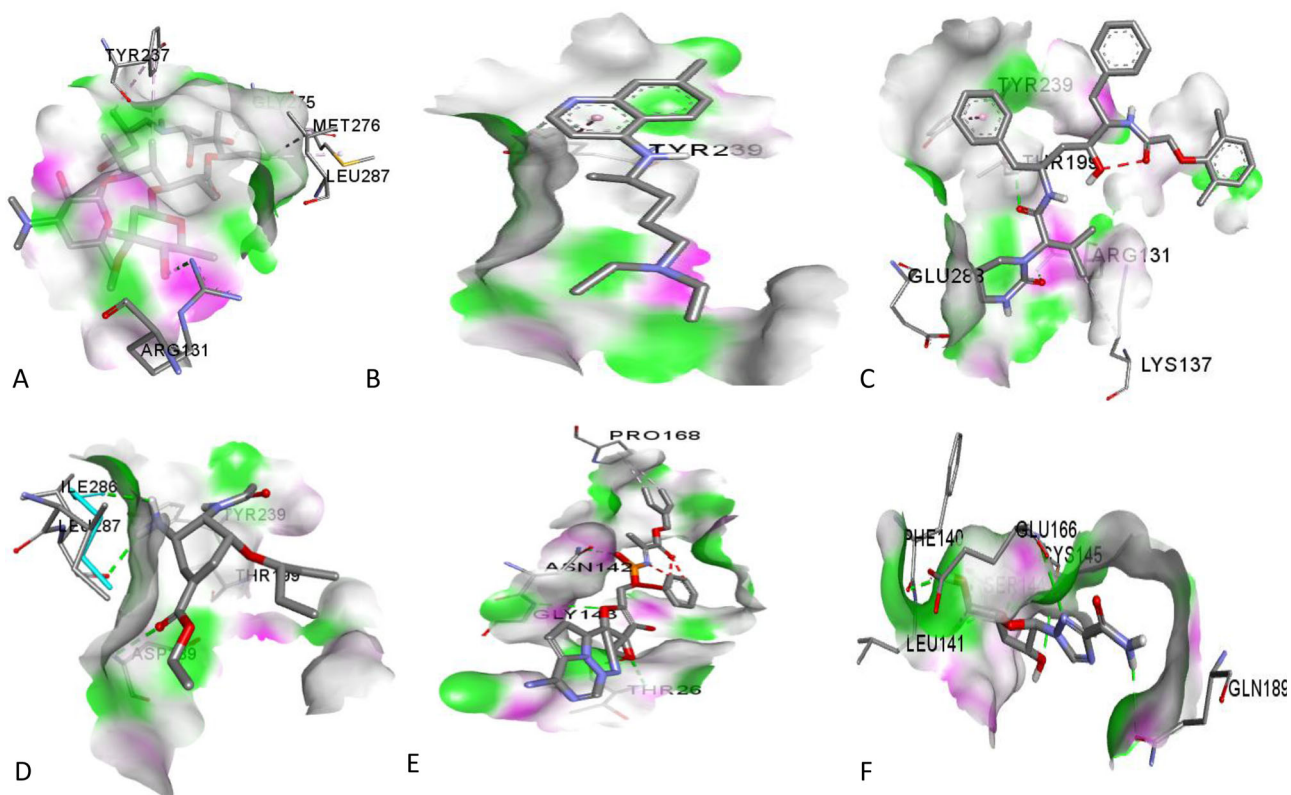


Figure 2. Docking view of the drugs in the binding sites of 3CLPro: (A) Azithromycin, (B) Chloroquine (C) Lopinavir (D) Oseltamivir, (E) Remdesivir, (F) Ribavirin.

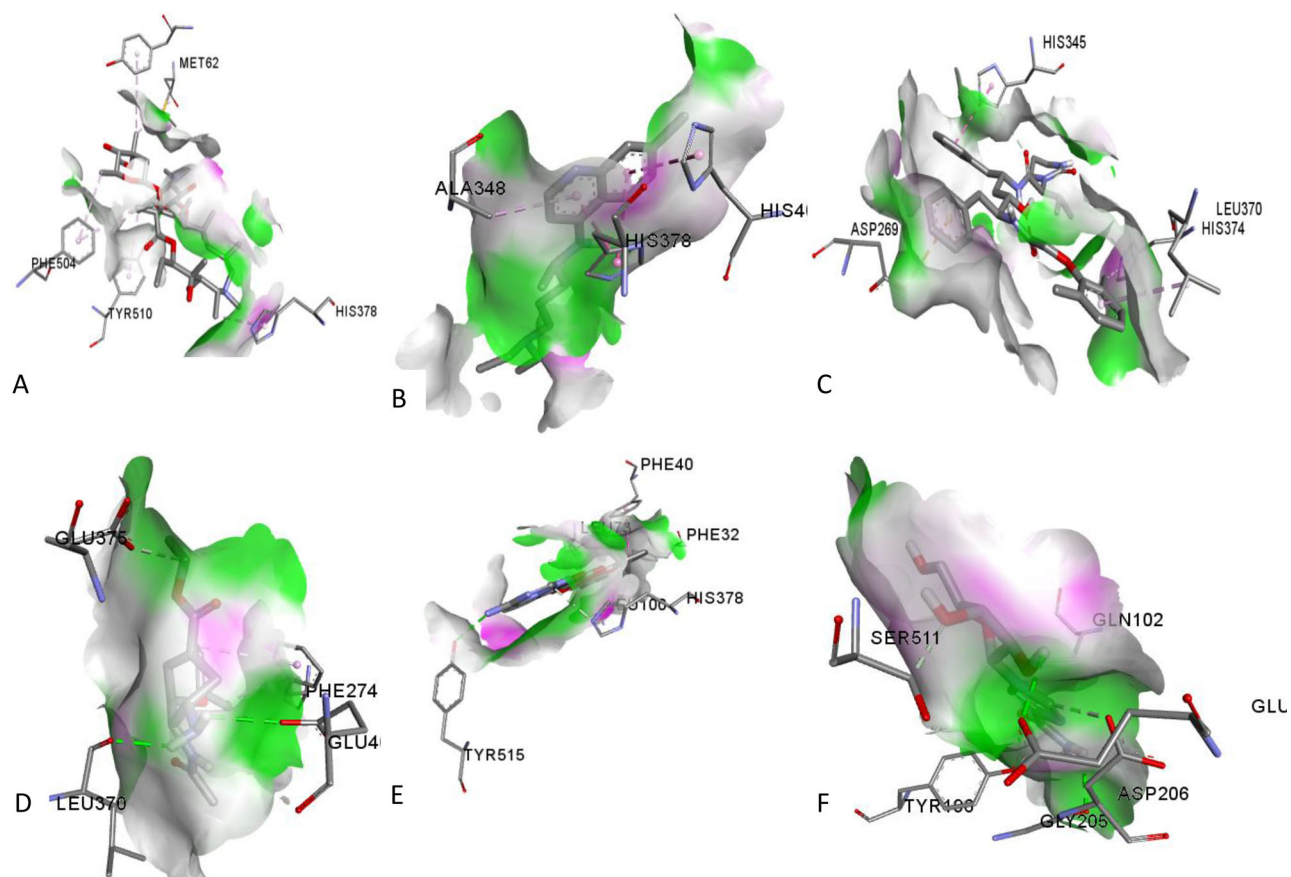


Figure 3. Docking view of the drugs in the binding sites of SARS COV-SPIKE GLYCO/ACE2: (A) Azithromycin, (B) Chloroquine (C) Lopinavir (D) Oseltamivir, (E) Remdesivir, (F) Ribavirin.

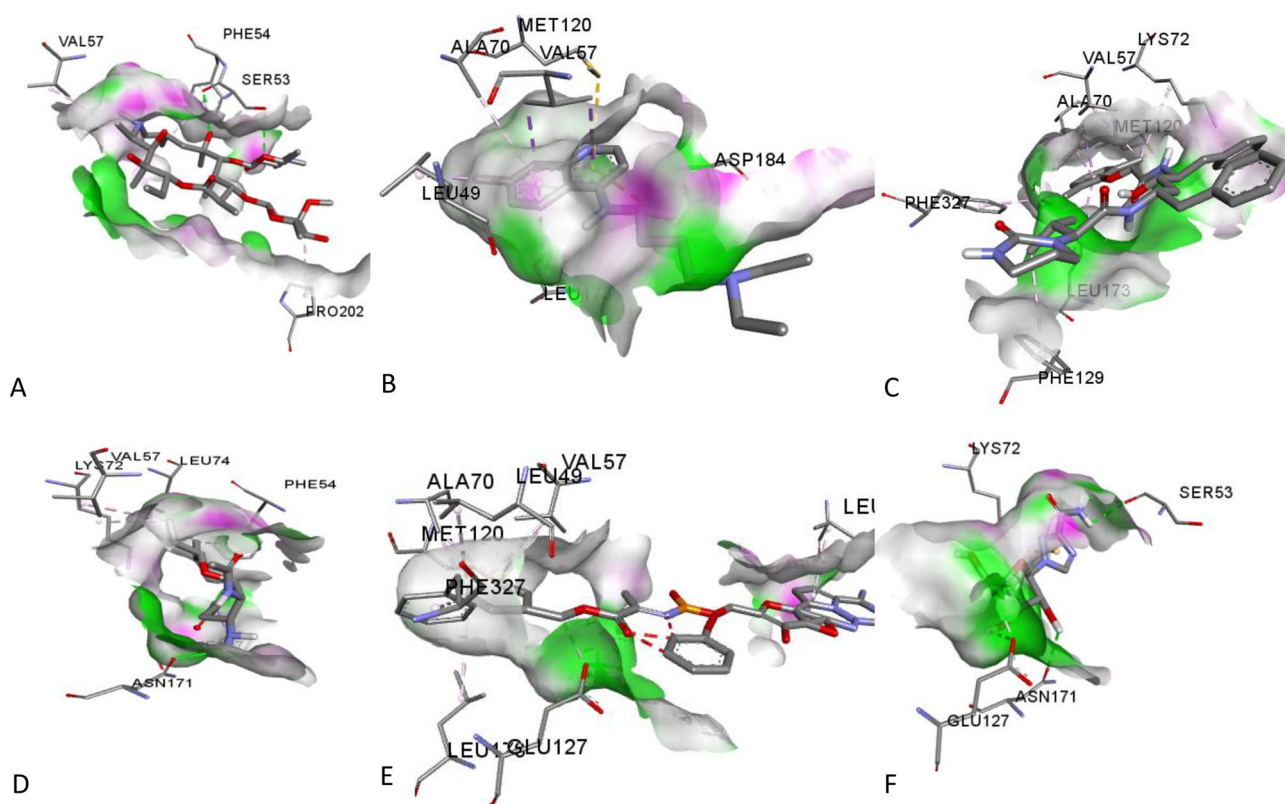


Figure 4. Docking view of the drugs in the binding sites of PKA: (A) Azithromycin, (B) Chloroquine (C) Lopinavir (D) Oseltamivir, (E) Remdesivir, (F) Ribavirin.

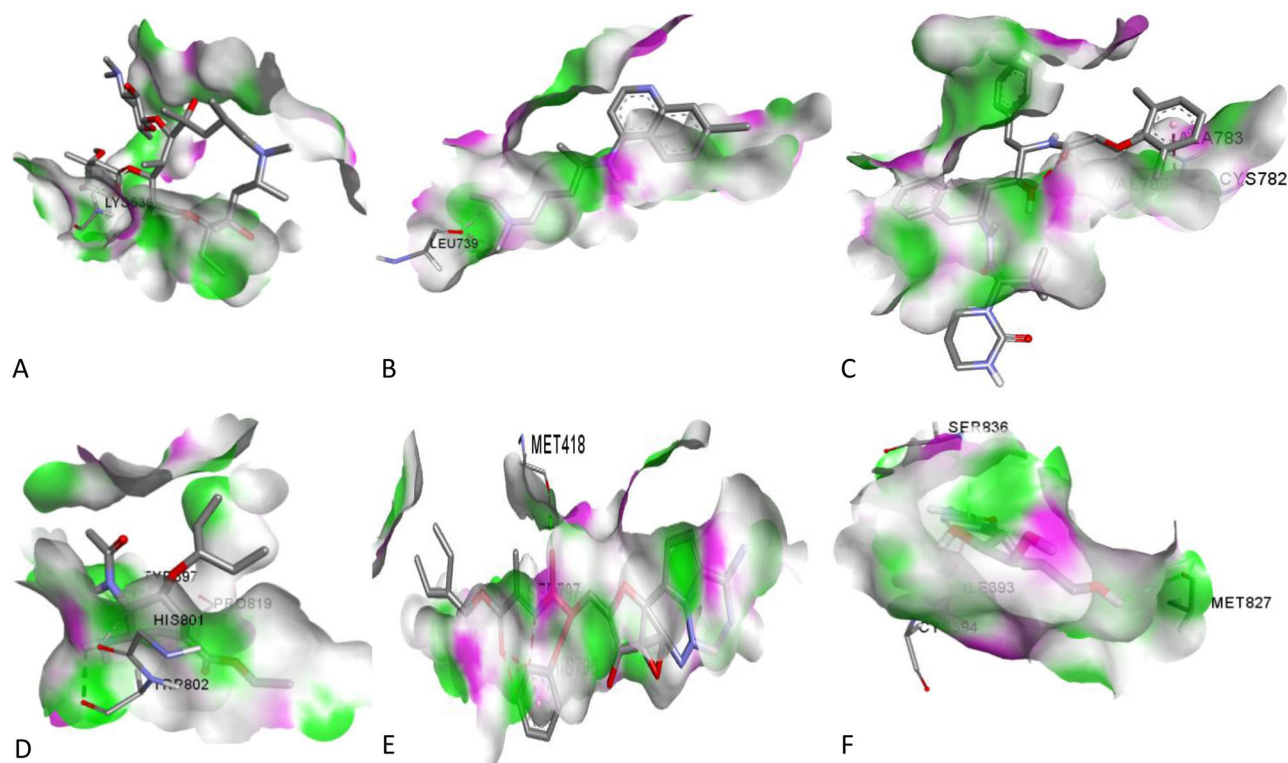


Figure 5. Docking view of the drugs in the binding sites of V-ATPase: (A) Azithromycin, (B) Chloroquine (C) Lopinavir (D) Oseltamivir, (E) Remdesivir, (F) Ribavirin.

the lysosomal pH gradient by increasing H^+ influx and consequent alkalinity. Moreover, the amino acids His401, Ala348, and His378 were predicted to be the key residues for chloroquine binding to human SARS-CoV spike glycoprotein/ACE-2 complex. Analysis of the results of the autodock software

revealed that chloroquine has a considerable binding affinity with coronavirus target protease.

The results of the molecular dynamics simulation of the docked complexes are presented in Figure 6. The deformability graphs of the complexes illustrated the degree of the

Table 8. Summary of ligand-amino acid interactions in various binding pockets.

S/N	Compounds	Plpro	3CLpro	SARS-CoV spike glycoprotein/ ACE-2 complex	cAMP-PKA	V-ATPase
1	Azithromycin	ASN157, ASP77A, ASP77B, ASN157C, HIS74 GLN175	TYR237, MET276, LEU287, ARG131, GLY275 TYR239	TYR510 PHE504, MET62, TYR50, HIS378 HIS401, ALA348, HIS378	PRO202, VAL57, PHE54, SER53 ALA70, LEU173, LEU49, VAL57, MET120, ASP184 PHE129, PHE327, LEU173, MET120, ALA70, LYS72, VAL57	LYS536
2	Chloroquine					LEU739
3	Lopinavir	TYR155, LUE76, VAL203, HIS90, HIS176	LYS137, ARG131, GLU288, THR199, TYR239	ASP269, LEU370, HIS374, HIS345		CYS782, PHE423
4	Oseltamivir	HIS90, ASN129, GLN175	ASP289, TYR239, LEU287, ILE286, THR199	GLU375, LEU370, GLU406, THR276, PHE274	PHE187, VAL57, LYS72, PHE54, LEU74, ASN171 LEU82, LU127, PHE327, LEU49, LEU172, MET120, ALA70, VAL57	PRO819, TRP802, TYR897, HIS801 MET422, HIS796
5	Remdesivir	LEU179, GLY202, SER86, ARG83, LEU76, PHE70, SER79	THR26, PRO168, ASN142, GLY143	HIS378, TYR515, LEU73, LEU100, PHE32, PHE40		
6	Ribavirin	THR201, HIS90, GLN175, GLU204	GLN189, CYS145, SER144, LEU141, PHE140, GLU166	GLN102, TYR196, GLY205, ASP206, GLU398, SER511	SER53, LYS72, ASN171, GLU127	MET827, SER836, ILE393

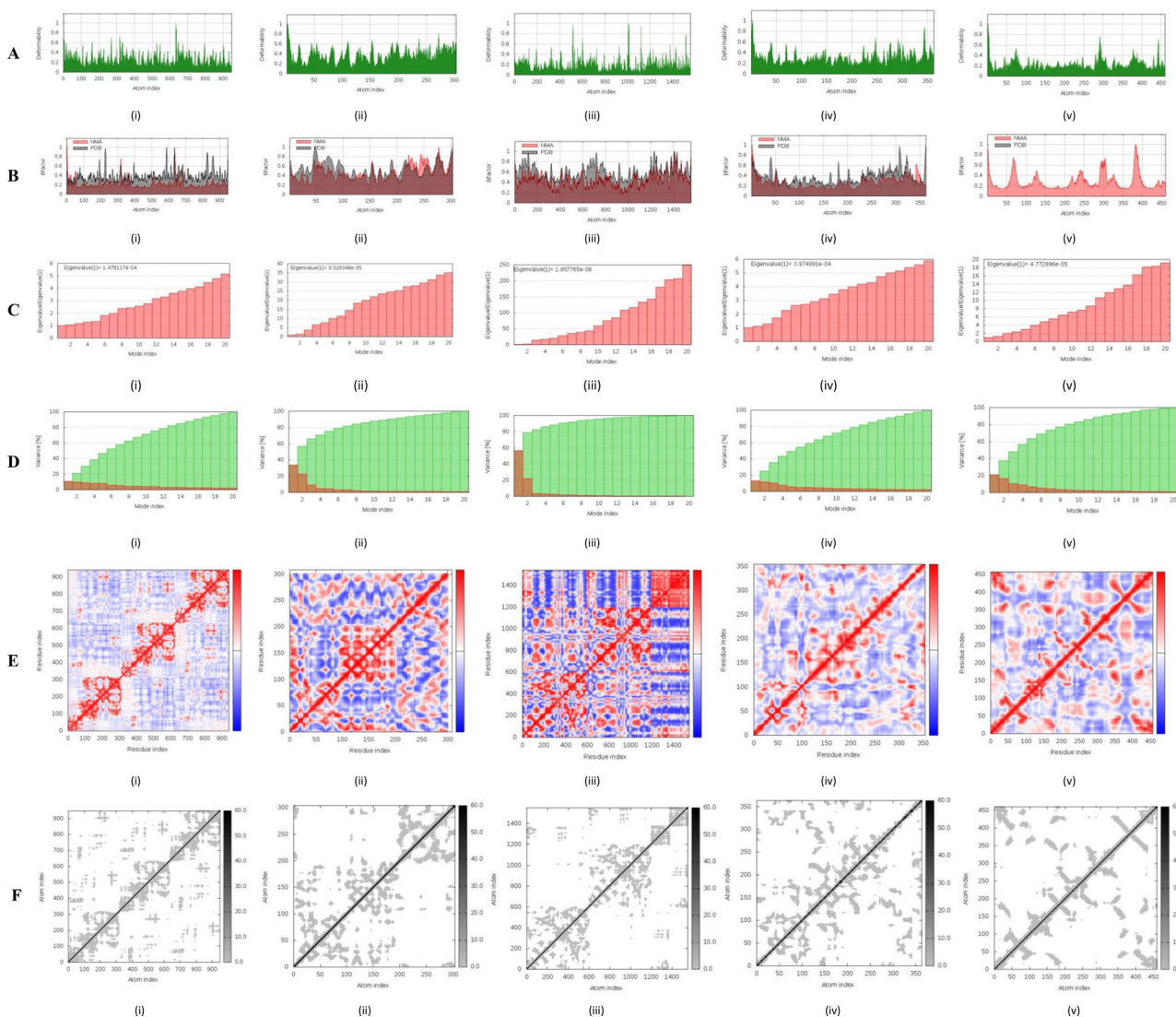


Figure 6. Molecular dynamics simulation showing (A) deformability, (B) B-factor, (C) eigenvalues, (D) variance, (E) covariance map (F) elastic network of (i) PLpro (ii) 3CLpro (iii) SARS-CoV spike glycoprotein/ACE-2 complex (iv) cAMP-PKA (v) V-ATPase docked complexes.

capability of the respective molecule to deform shown by the peaks (Figure 6A). The empirical B-factor graphs of the complexes presented in Figure 6B were obtained from the corresponding PDB field and NMA mobility. The computed eigenvalues of the docked complexes that characterise the motion stiffness and the movement of the proteins are shown in Figure 6C with SARS-CoV spike glycoprotein/ACE-2 complex predicted to having comparatively the least required energy to deform its structure based on the lowest eigenvalue. However, the associated variance is inversely related to the eigenvalue with the individual variance indicated by red coloured bars and cumulative variance indicated by green coloured bars (Figure 6D) while the coupling between pairs of residues is illustrated by the co-variance map (Figure 6E) where red colour showed the correlated motion between a pair of residues, white colour indicated uncorrelated motion and the anti-correlated motion was indicated by blue colour. The elastic network model illustrated by the elastic map (Figure 6F) expresses the connection between the atoms with indicated by 'dot' and the colour

gradient of the dot is directly related to their stiffness, thus, darker 'spot' designate stiffer springs (López-Blanco et al., 2014).

4. Conclusion

All the antiviral drugs had binding affinities for SARS spike glycoprotein-human angiotensin-converting enzyme 2 and SARS-CoV main protease. Out of the five already established antiviral drugs, lopinavir had the highest binding affinity towards SARS-CoV protease while ribavirin had the lowest binding affinity. Chloroquine recently discovered for the treatment of Coronavirus also had a considerable binding affinity to the pocket site of SARS spike glycoprotein-human angiotensin-converting enzyme 2 and SARS-CoV main protease. Binding of these drugs could interfere or inhibit the functions of coronavirus thereby preventing its cellular entry and proliferation. Although chloroquine could bind to the selected target proteins/enzymes, the result shows it could not be as effective as others. However, coupling it with

metals could improve its binding affinity. Oseltamivir, azithromycin, and ribavirin, when compared to chloroquine, showed good drug-likeness based on the predicted pharmacokinetic and pharmacodynamics properties as revealed by low CYP inhibitory promiscuity and relatively low toxicity. However, further experimental works are recommended to validate the effectiveness of the identified therapeutic agents.

Authors contribution

AOA, BJO, and IFO initiated and designed the study; all the authors were involved in the analyses and interpretations of data. All authors wrote and approved the final manuscript.

Disclosure statement

No potential conflict of interest was reported by the authors.

ORCID

Babatunde Joseph Oso  <http://orcid.org/0000-0001-8667-7108>

References

- Aanouz, I., Belhassan, A., El Khatabi, K., Lakhlifi, T., El Idrissi, M., & Bouachrine, M. (2020). Moroccan medicinal plants as inhibitors of COVID-19: Computational investigations. *Journal of Biomolecular Structure and Dynamics*. <https://doi.org/10.1080/07391102.2020.1758790>
- Adeoye, A. O., Olanlokun, J. O., Tijani, H., Lawal, S. O., Babarinde, C. O., Akinwale, M. T., & Bewaji, C. O. (2019). Molecular docking analysis of apigenin and quercetin from ethyl acetate fraction of *Adansonia digitata* with malaria-associated calcium transport protein: An in silico approach. *Heliyon*, 5(9), e02248. <https://doi.org/10.1016/j.heliyon.2019>
- Arabi, Y. M., Balkhy, H. H., Hayden, F. G., Bouchama, A., Luke, T., Baillie, J. K., Al-Omari, A., Hajeer, A. H., Senga, M., Denison, M. R., Nguyen-Van-Tam, J. S., Shindo, N., Bermingham, A., Chappell, J. D., Van Kerkhove, M. D., & Fowler, R. A. (2017). Middle East respiratory syndrome. *The New England Journal of Medicine*, 376(6), 584–594. <https://doi.org/10.1056/NEJMs1408795>
- Berman, H. M., Westbrook, J., Feng, Z., Gilliland, G., Bhat, T. N., Weissig, H., Shindyalov, I. N., & Bourne, P. E. (2000). The protein data bank. *Nucleic Acids Research*, 28(1), 235–242. <https://doi.org/10.1093/nar/28.1.235>
- Boopathi, S., Poma, A. B., & Kolandaivel, P. (2020). Novel 2019 coronavirus structure, mechanism of action, antiviral drug promises and rule out against its treatment. *Journal of Biomolecular Structure and Dynamics*. <https://doi.org/10.1080/07391102.2020.1758788>
- Chen, F., Liu, H., Sun, H. Y., Pan, P. C., Li, Y. Y., Li, D., & Hou, T. J. (2016). Assessing the performance of the MM/PBSA and MM/GBSA methods. 6. Capability to predict protein-protein binding free energies and re-rank binding poses generated by protein-protein docking. *Physical Chemistry Chemical Physics*, 18(32), 22129–22139. doi: [10.1039/c6cp03670h](https://doi.org/10.1039/c6cp03670h)
- Cheng, F., Li, W., Zhou, Y., Shen, J., Wu, Z., Liu, G., Lee, P. W., & Tang, Y. (2012). admetSAR: A comprehensive source and free tool for assessment of chemical ADMET properties. *Journal of Chemical Information and Modeling*, 52(11), 3099–3105. <https://doi.org/10.1021/acs.jcim.9b00969>
- Cheng, F., Yu, Y., Zhou, Y., Shen, Z., Xiao, W., Liu, G., Li, W., Lee, P. W., & Tang, Y. (2011). Insights into molecular basis of cytochrome p450 inhibitory promiscuity of compounds. *Journal of Chemical Information and Modeling*, 51(10), 2482–2495. <https://doi.org/10.1021/ci200317s>
- Cleri, D. J., Ricketti, A. J., & Vernaleo, J. R. (2010). Severe acute respiratory syndrome (SARS). *Infectious Disease Clinics of North America*, 24(1), 175–202. <https://doi.org/10.1016/j.idc.2009.10.005>
- de Haan, C. A., Stadler, K., Godeke, G. J., Bosch, B. J., & Rottier, P. J. (2004). Cleavage inhibition of the murine coronavirus spike protein by a furin-like enzyme affects cell-cell but not virus-cell fusion. *Journal of Virology*, 78(11), 6048–6054. <https://doi.org/10.1128/JVI.00074-08>
- Elfiky, A. A., & Azzam, E. B. (2020). Novel guanosine derivatives against MERS CoV polymerase: An in silico perspective. *Journal of Biomolecular Structure and Dynamics*. <https://doi.org/10.1080/07391102.2020.1758789>
- Elmezayen, A. D., Al-Obaidi, A., Şahin, A. T., & Yelekcı, K. (2020). Drug repurposing for coronavirus (COVID-19): In silico screening of known drugs against coronavirus 3CL hydrolase and protease enzymes. *Journal of Biomolecular Structure and Dynamics*. <https://doi.org/10.1080/07391102.2020.1758791>
- Elokely, K. M., & Doerkse, R. J. (2013). Docking challenge: Protein sampling and molecular docking performance. *Journal of Chemical Information and Modeling*, 53(8), 1934–1945. <https://doi.org/10.1021/ci400040d>
- Enayatkhani, M., Hasaniazad, M., Faezi, S., Guklani, H., Davoodian, P., Ahmadi, N., Einakian, M. A., Karmostaji, A., & Ahmadi, K. (2020). Reverse vaccinology approach to design a novel multi-epitope vaccine candidate against COVID-19: An in silico study. *Journal of Biomolecular Structure and Dynamics*. <https://doi.org/10.1080/07391102.2020.1756411>
- Enmozhi, S. K., Raja, K., Sebastine, I., & Joseph, J. (2020). Andrographolide as a potential inhibitor of SARS-CoV-2 main protease: An in silico approach. *Journal of Biomolecular Structure and Dynamics*. <https://doi.org/10.1080/07391102.2020.1760136>
- Gay, B., Bernard, E., Solignat, M., Chazal, N., Devaux, C., & Briant, L. (2012). pH-dependent entry of Chikungunya virus into *Aedes albopictus* cells. *Infection, Genetics and Evolution: Journal of Molecular Epidemiology and Evolutionary Genetics in Infectious Diseases*, 12(6), 1275–1281. <https://doi.org/10.1016/j.meegid.2012.02.003>
- Gupta, M. K., Vemula, S., Donde, R., Gouda, G., Behera, L., & Vadde, R. (2020). In-silico approaches to detect inhibitors of the human severe acute respiratory syndrome coronavirus envelope protein ion channel. *Journal of Biomolecular Structure and Dynamics*. <https://doi.org/10.1080/07391102.2020.1751300>
- Hasan, A., Paray, B. A., Hussain, A., Qadir, F. A., Attar, F., Aziz, F. M., Sharifi, M., Derakhshankhah, H., Rasti, B., Mehrabi, M., Shahpasand, K., Aa, S., & Falahati, M. (2020). A review on the cleavage priming of the spike protein on coronavirus by angiotensin-converting enzyme-2 and furin. *Journal of Biomolecular Structure and Dynamics*. <https://doi.org/10.1080/07391102.2020.1754293>
- Haworth, R. S., McCann, C., Snabaitis, A. K., Roberts, N. A., & Avkiran, M. (2003). Stimulation of the plasma membrane Na⁺/H⁺ exchanger NHE1 by sustained intracellular acidosis. Evidence for a novel mechanism mediated by the ERK pathway. *The Journal of Biological Chemistry*, 278(34), 31676–31684. <https://doi.org/10.1074/jbc.M304400200>
- Hughes, J. D., Blagg, J., Price, D. A., Bailey, S., Decrescenzo, G. A., Devraj, R. V., Ellsworth, E., Fobian, Y. M., Gibbs, M. E., Gilles, R. W., Greene, N., Huang, E., Krieger-Burke, T., Loesel, J., Wager, T., Whiteley, L., & Zhang, Y. (2008). Physicochemical drug properties associated with in vivo toxicological outcomes. *Bioorganic & Medicinal Chemistry Letters*, 18(17), 4872–4875. <https://doi.org/10.1016/j.bmcl.2007.07.071>
- Hui, D. S., I Azhar, E., Madani, T. A., Ntoumi, F., Kock, R., Dar, O., Ippolito, G., Mchugh, T. D., Memish, Z. A., Drosten, C., Zumla, A., & Petersen, E. (2020). The continuing 2019-nCoV epidemic threat of novel coronaviruses to global health - The latest 2019 novel coronavirus outbreak in Wuhan, China. *International Journal of Infectious Diseases: Official Publication of the International Society for Infectious Diseases*, 91, 264–266. <https://doi.org/10.1016/j.ijid.2020.01.009>
- Huotari, J., & Helenius, A. (2011). Endosome maturation. *The EMBO Journal*, 30(17), 3481–3500. <https://doi.org/10.1038/emboj.2011.286>
- Ishida, Y., Nayak, S., Mindell, J. A., & Grabe, M. (2013). A model of lysosomal pH regulation. *The Journal of General Physiology*, 141(6), 705–720. <https://doi.org/10.1085/jgp.201210930>
- Joshi, R. S., Jagdale, S. S., Bansode, S. B., Shankar, S. S., Tellis, M. B., Pandya, V. K., Chugh, A., Giri, A. P., & Kulkarni, M. J. (2020). Discovery of potential multi-target-directed ligands by targeting host-specific

- SARS-CoV-2 structurally conserved main protease. *Journal of Biomolecular Structure and Dynamics*. <https://doi.org/10.1080/07391102.2020.1760137>
- Khan, R. J., Jha, R. K., Amera, G. M., Jain, M., Singh, E., Pathak, A., Singh, R. P., M. J., & Singh, A. K. (2020a). Targeting SARS-CoV-2: A systematic drug repurposing approach to identify promising inhibitors against 3C-like proteinase and 2'-O-ribose methyltransferase. *Journal of Biomolecular Structure and Dynamics*. <https://doi.org/10.1080/07391102.2020.1753577>
- Khan, S. A., Zia, K., Ashraf, S., Uddin, R., & Ul-Haq, Z. (2020b). Identification of chymotrypsin-like protease inhibitors of SARS-CoV-2 via integrated computational approach. *Journal of Biomolecular Structure and Dynamics*. <https://doi.org/10.1080/07391102.2020.1751298>
- Kim, S., Chen, J., Cheng, T., Gindulyte, A., He, J., He, S., Li, Q., Shoemaker, B. A., Thiessen, P. A., Yu, B., Zaslavsky, L., Zhang, J., & Bolton, E. E. (2019). PubChem 2019 update: Improved access to chemical data. *Nucleic Acids Research*, 47(D1), D1102–D1109. <https://doi.org/10.1093/nar/gky1033>
- Larregieu, C. A., & Benet, L. Z. (2013). Drug discovery and regulatory considerations for improving *in silico* and *in vitro* predictions that use Caco-2 as a surrogate for human intestinal permeability measurements. *The AAPS Journal*, 15(2), 483–497. <https://doi.org/10.1208/s12248-013-9456-8>
- Li, W., Moore, M. J., Vasilieva, N., Sui, J., Wong, S. K., Berne, M. A., Somasundaran, M., Sullivan, J. L., Luzuriaga, K., Greenough, T. C., Choe, H., & Farzan, M. (2003). Angiotensin-converting enzyme 2 is a functional receptor for the SARS coronavirus. *Nature*, 426(6965), 450–454. <https://doi.org/10.1038/nature02145>
- Lipinski, C. A., Lombardo, F., Dominy, B. W., & Feeney, P. J. (1997). Experimental and computational approaches to estimate solubility and permeability in drug discovery and development settings. *Advanced Drug Delivery Reviews*, 23(1–3), 3–25. 1997, [https://doi.org/10.1016/S0169-409X\(96\)00423-1](https://doi.org/10.1016/S0169-409X(96)00423-1)
- López-Blanco, J. R., Aliaga, J. I., Quintana-Ortí, E. S., & Chacón, P. (2014). iMODS: Internal coordinates normal mode analysis server. *Nucleic Acids Research*, 42(Web Server issue), W271–276. <https://doi.org/10.1093/nar/gku339>
- Muralidharan, N., Sakthivel, R., Velmurugan, D., & Gromiha, M. M. (2020). Computational studies of drug repurposing and synergism of lopinavir, oseltamivir and ritonavir binding with SARS-CoV-2 protease against COVID-19. *Journal of Biomolecular Structure and Dynamics*. <https://doi.org/10.1080/07391102.2020.1752802>
- Nakamura, N., Tanaka, S., Teko, Y., Mitsui, K., & Kanazawa, H. (2005). Four Na⁺/H⁺ exchanger isoforms are distributed to Golgi and post-Golgi compartments and are involved in organelle pH regulation. *The Journal of Biological Chemistry*, 280(2), 1561–1572. <https://doi.org/10.1074/jbc.M410041200>
- Nukoolkarn, V., Lee, V. S., Malaisree, M., Aruksakulwong, O., & Hannongbua, S. (2008). Molecular dynamic simulations analysis of ritonavir and lopinavir as SARS-CoV 3CL(pro) inhibitors. *Journal of Theoretical Biology*, 254(4), 861–867. <https://doi.org/10.1016/j.jtbi.2008.07.030>
- O'Boyle, N. M., Banck, M., James, C. A., Morley, C., Vandermeersch, T., & Hutchison, G. R. (2011). Open babel: An open chemical toolbox. *Journal of Cheminformatics*, 3(10), 33. <https://doi.org/10.1186/1758-2946-3-33>
- Oso, B. J., & Olaoye, I. F. (2020). Comparative *in vitro* studies of antiglycemic potentials and molecular docking of *Ageratum conyzoides* L. and *Phyllanthus amarus* L. methanolic extracts. *SN Applied Sciences*, 2(4), 629. <https://doi.org/10.1007/s42452-020-2275-5>
- Oso, B. J., Oyewo, E. B., & Oladiji, A. T. (2019). Influence of ethanolic extracts of dried fruit of *Xylopiasaeethiopia* (Dunal) A. Rich on haematological and biochemical parameters in healthy Wistar rats. *Clinical Phytoscience*, 5(1), 9. <https://doi.org/10.1186/s40816-019-0104-4>
- Pant, S., Singh, M., Ravichandiran, V., Murty, U. S. N., & Srivastava, H. K. (2020). Peptide-like and small-molecule inhibitors against Covid-19. *Journal of Biomolecular Structure and Dynamics*. <https://doi.org/10.1080/07391102.2020.1757510>
- Park, J. E., Cruz, D. J., & Shin, H. J. (2014). Clathrin- and serine protease-dependent uptake of porcine epidemic diarrhea virus into Vero cells. *Virus Research*, 191, 21–29. <https://doi.org/10.1016/j.virusres.2014.07.022>
- Paules, C. I., Marston, H. D., & Fauci, A. S. (2020). Coronavirus infections—more than just the common cold. *JAMA*, 323(8), 707–708. <https://doi.org/10.1001/jama.2020.0757>
- Pires, D. E. V., Blundell, T. L., & Ascher, D. B. (2015). pkCSM: Predicting small-molecule pharmacokinetic and Toxicity Properties Using Graph-Based Signatures. *Journal of Medicinal Chemistry*, 58(9), 4066–4072. <https://doi.org/10.1021/acs.jmedchem.5b00104>
- Plempner, R. K. (2011). Cell entry of enveloped viruses. *Current Opinion in Virology*, 1(2), 92–100. <https://doi.org/10.1016/j.coviro.2011.06.002>
- Prasad, H., & Rao, R. (2015). The Na⁺/H⁺ exchanger NHE6 modulates endosomal pH to control processing of amyloid precursor protein in a cell culture model of Alzheimer disease. *The Journal of Biological Chemistry*, 290(9), 5311–5327. <https://doi.org/10.1074/jbc.M114.602219>
- Richards, A. L., & Jackson, W. T. (2012). Intracellular vesicle acidification promotes maturation of infectious poliovirus particles. *PLoS Pathogens*, 8(11), e1003046. <https://doi.org/10.1371/journal.ppat.1003046>
- Sarma, P., Sekhar, N., Prajapat, M., Avti, P., Kaur, H., Kumar, S., Singh, S., Kumar, H., Prakash, A., Dp, D., & Medhi, B. (2020). In-silico homology assisted identification of inhibitor of RNA binding against 2019-nCoV N-protein (N terminal domain). *Journal of Biomolecular Structure and Dynamics*. <https://doi.org/10.1080/07391102.2020.1753580>
- Skariyachan, S., Challapilli, S. B., Packirisamy, S., Kumargowda, S. T., & Sridhar, V. S. (2019). Recent aspects on the pathogenesis mechanism, animal models and novel therapeutic interventions for Middle East respiratory syndrome coronavirus infections. *Frontiers in Microbiology*, 10, 569. <https://doi.org/10.3389/fmicb.2019.00569>
- Slesiona, S., Gressler, M., Mihlan, M., Zaehle, C., Schaller, M., Barz, D., Hube, B., Jacobsen, I. D., & Brock, M. (2012). Persistence versus escape: *Aspergillus terreus* and *Aspergillus fumigatus* employ different strategies during interactions with macrophages. *PLoS One*, 7(2), e31223. <https://doi.org/10.1371/journal.pone.0031223>
- Srivalli, K. M., & Lakshmi, P. K. (2012). Overview of P-glycoprotein inhibitors: A rational outlook. *Brazilian Journal of Pharmaceutical Sciences*, 48(3), 353–367. <https://doi.org/10.1590/S1984-82502012000300002>
- Trott, O., & Olson, A. J. (2010). AutoDock Vina: Improving the speed and accuracy of docking with a new scoring function, efficient optimization, and multithreading. *Journal of Computational Chemistry*, 31(2), 455–461. <https://doi.org/10.1002/jcc.21334>
- Vincent, M. J., Bergeron, E., Benjannet, S., Erickson, B. R., Rollin, P. E., Ksiazek, T. G., Seidah, N. G., & Nichol, S. T. (2005). Chloroquine is a potent inhibitor of SARS coronavirus infection and spread. *Virology Journal*, 2, 69. <https://doi.org/10.1186/1743-422X-2-69>
- Wang, S., Li, Y., Wang, J., Chen, L., Zhang, L., Yu, H., & Hou, T. (2012). ADMET evaluation in drug discovery. 12. Development of binary classification models for prediction of hERG potassium channel blockage. *Molecular Pharmaceutics*, 9(4), 996–1010. <https://doi.org/10.1021/mp300023x>
- Williams, J. A., Hyland, R., Jones, B. C., Smith, D. A., Hurst, S., Goosen, T. C., Peterkin, V., Koup, J. R., & Ball, S. E. (2004). Drug-drug interactions for UDP-glucuronosyltransferase substrates: A pharmacokinetic explanation for typically observed low exposure (AUCi/AUC) ratios. *Drug Metabolism and Disposition*, 32(11), 1201–1208. <https://doi.org/10.1124/dmd.104.000794>
- Yazdaniyan, M., Glynn, S. L., Wright, J. L., & Hawi, A. (1998). Correlating partitioning and caco-2 cell permeability of structurally diverse small molecular weight compounds. *Pharmaceutical Research*, 15(9), 1490–1494. <https://doi.org/10.1023/A:1011930411574>
- Zhao, H., Wiederkehr, M. R., Fan, L., Collazo, R. L., Crowder, L. A., & Moe, O. W. (1999). Acute Inhibition of Na/H Exchanger NHE-3 by cAMP. Role of Protein Kinase A and NHE-3 Phosphoserines 552 and 605. *Journal of Biological Chemistry*, 274(7), 3978–3987. <https://doi.org/10.1074/jbc.274.7.3978>
- Zumla, A., Hui, D. S., & Perlman, S. (2015). Middle East respiratory syndrome. *The Lancet*, 386(9997), 995–1007. [https://doi.org/10.1016/S0140-6736\(15\)60454-8](https://doi.org/10.1016/S0140-6736(15)60454-8)